Organic Electronics 13 (2012) 425–431

Contents lists available at SciVerse ScienceDirect

Organic Electronics

journal homepage: www.elsevier.com/locate/orgel

Letter

Enhanced performance of dye-sensitized solar cells with novel 2,6-diphenyl-4*H*-pyranylidene dyes

Altan Bolag [a], Jun-ichi Nishida [a], Kohjiro Hara [b], Yoshiro Yamashita [a,*]

[a] Department of Electronic Chemistry, Tokyo Institute of Technology, G1-8, 4259 Nagatsuta-cho, Midori-ku, Yokohama, Kanagawa 226-8502, Japan
[b] Advanced Organic Materials Team, Research Center for Photovoltaics, Advanced Industrial Science and Technology, Central 5, 1-1-1 Higashi, Tsukuba, Ibaraki 305-8565, Japan

ARTICLE INFO

Article history:
Received 5 July 2011
Received in revised form 4 October 2011
Accepted 21 November 2011
Available online 17 December 2011

Keywords:
Dye-sensitized solar cell
Organic sensitizer
Diphenylpyranylidene

ABSTRACT

Novel 2,6-diphenyl-4*H*-pyranylidene derivatives were designed and synthesized as dyes for dye-sensitized solar cells (DSSC). Dyes **2a**, **b** with a phenyl substituent showed high DSSC energy conversion efficiencies of 5.3% (J_{sc} = 10.3 mA/cm^2, V_{oc} = 0.72 V, FF = 0.72) and 4.7% (J_{sc} = 8.9 mA/cm^2, V_{oc} = 0.73 V, FF = 0.72) at 100 mW/cm^2 under simulated AM 1.5 G solar light conditions. These values are twice better than that of dye **1** without the phenyl substituent under the same conditions. Both the photocurrent density (J_{sc}) and open circuit voltage (V_{oc}) of DSSCs based on dyes **2a**, **b** are increased compared with **1**. It can be attributed to their twisted structures, absorption abilities and proper energy levels. This result shows that the tetraphenylpyranylidene is a promising electron-donor unit for high-efficiency DSSCs.

1. Introduction

The use of solar cells is becoming important for the global energy demand because of their inexhaustible supply and pollution-free properties. In recent years, dye-sensitized solar cells (DSSCs) have attracted increasing interest in the photovoltaics research due to their appealing advantages such as low manufacturing cost, flexibility and lightweight, which are satisfying the needs in the new energy utilization and allow them to compete with traditional photovoltaic devices [1–3]. Dyes used for DSSCs can be mainly divided into organic-metal complexes and pure organic dyes. Metal complex dyes show higher performances and energy conversion efficiencies over 11–12% have been reported for ruthenium sensitizers [2]. On the other hand, pure organic dyes have advantages such as larger molar extinction coefficients, easier preparation, more controllable energy levels and environmentally friendly properties. Although efficiencies of DSSCs with metal-free organic dyes have been improved over the past decades [3], developing novel organic sensitizers is still in demand for achieving higher efficiencies of DSSCs as well as for investigating the dye structure-performance relationship. According to our previous studies, 2,6-diphenyl-4*H*-pyranylidenes have intense absorptions in the visible region as well as proper energy levels, and the derivative **1** was successfully used as dye of DSSCs for the first time [4]. However, as reported, the incident photo-to-current conversion efficiency (IPCE) of the dye was lower than 60%, which was attributed to the planar structure of diphenylpyranylidene unit resulting in dye-aggregation on TiO_2 thin film. Furthermore, the derivative **1** undergoes a dimerization reaction upon electrochemical oxidation [5], which may also result in low efficiency. In order to overcome these points, substituents were introduced at the vinyl position to give novel diphenylpyranylidene dyes **2a–c** as shown in Fig. 1. We present herein the synthesis, physical properties and DSSC device performances of **2a–c** with a phenyl or methyl group at the vinyl position.

* Corresponding author. Tel.: +81 45 924 5571; fax: +81 45 924 5489.
E-mail address: yoshiro@echem.titech.ac.jp (Y. Yamashita).

1566-1199/$ - see front matter © 2011 Elsevier B.V. All rights reserved.
doi:10.1016/j.orgel.2011.11.020

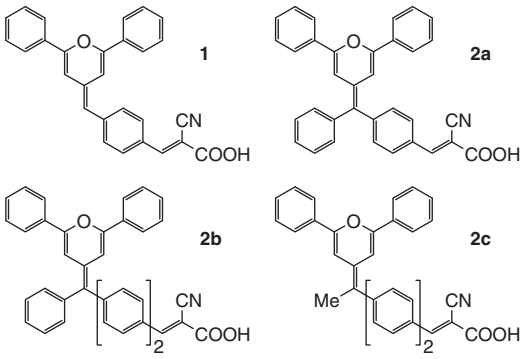

Fig. 1. Molecule structures of dyes **1** and **2a–c**.

2. Results and discussion

2.1. Synthesis

The synthesis was accomplished as shown in Scheme 1. The diphenylpyranylidene unit was introduced by the Wittig reaction of tributyl(2,6-diphenyl-4*H*-pyran-4-yl)phosphonium tetrafluoroborate [4] with benzophenone or acetophenone derivatives.

2.2. DFT calculations

The molecular orbital calculations for **2a–c** were carried out using Gaussian 03 program at the B3LYP/6-31G(d) level in comparison with **1**. The results are shown in Fig. 2.

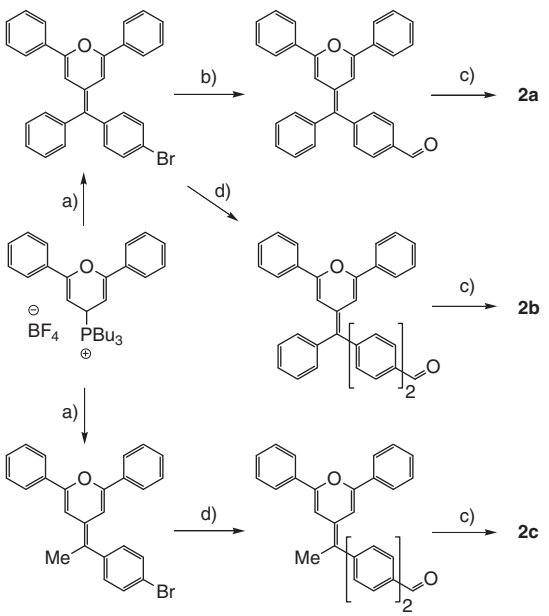

Scheme 1. Synthesis of diphenylpyranylidene derivatives. Reagents: (a) 4-bromobenzophenone or 4-bromoacetophenone, *n*-BuLi, dry THF. (b) *n*-BuLi, DMF, dry THF. (c) 2-Cyanoacetic acid, piperidine, MeCN. (d) (4-Formylphenyl)boronic acid, $Pd(PPh_3)_4$, Na_2CO_3, toluene, ethanol, H_2O.

The highest occupied molecular orbitals (HOMO) of these dyes exist on the diphenylpyranylidene moieties and phenyl/methyl group introduced at the vinyl position; the lowest unoccupied molecular orbitals (LUMO) of these dyes are mainly distributed over the cyanoacrylic acid part. Compared with **2b**, **c**, the LUMO is obviously extended over the diphenylpyranylidene unit in dye **2a**. The calculated HOMO–LUMO energy gap of **2a** becomes narrower than that of **1** due to the newly introduced phenyl group and that of **2b** is further decreased owing to the longer distance between the donor and acceptor parts by the biphenyl spacer (Table S1). The dihedral angles between the pyran and phenyl groups adjacent to the cyanoacrylic acid of **2a–c** are larger than that of **1** by 22–25°. On the other hand, the phenyl group at the vinyl position of **2a**, **b** gives dihedral angles of 59 and 57° with the pyran ring, respectively, indicating that **2a**, **b** are more twisted than **1**. On the basis of these results, introduction of phenyl/methyl group at the vinyl position is expected to give rise to larger steric interactions, which would lead to less dye-aggregation on the TiO_2 thin film, resulting in enhanced DSSCs device performances.

2.3. Photophysical and electrochemical properties

The UV–vis absorption spectra of dyes **2a–c** measured in dichloromethane are shown in Fig. 3a, and the data are presented in Table 1. Dye **2a** shows the absorption maximum in the visible region around 439 nm with a molar extinction coefficient of $1.7 \times 10^4\ M^{-1}\,cm^{-1}$, arising from an intramolecular charge transfer (CT) transition. The CT transition of dyes **2b**, **c** appears at the similar wavelengths to that of **2a** and their molar extinction coefficients are a little decreased to be 1.7×10^4 and $1.2 \times 10^4\ M^{-1}\,cm^{-1}$, respectively. Although the CT absorption maximum of **1** is red-shifted by 58–64 nm compared to those of **2a–c**, its absorption edge appears at the similar wavelength of 610 nm. The red-shift may be due to the more planar structure of **1** in solution. The molar extinction coefficients of the π–π^* transition observed at 352 and 349 nm for **2b**, **c**, respectively, are larger than that of dye **2a** at 295 nm due to the biphenyl spacer. The same phenomenon has been observed for other organic dyes when the π-conjugation of spacer is extended [6].

The UV–vis absorption spectra of dyes **2a–c** on TiO_2 thin films are shown in Fig. 3b. The TiO_2 films were immersed into the toluene solution of dyes (0.3 mM) overnight. The absorption of the blank TiO_2 film was subtracted from the curve. The absorption of dye **1** is 68 nm blue-shifted from 497 nm in the solution to 429 nm on the TiO_2 thin film. Considering the planar structure of dye **1**, the formation of H-aggregates on the TiO_2 surface may greatly contribute to the blue shift of the absorption spectra. In contrast, the absorptions of dyes **2a**, **b** are 6 nm shifted from 439 and 436 nm in the solution to 445 and 442 nm on the TiO_2 thin film. These slight shifts of absorption spectra imply that the twisted molecules of dyes **2a**, **b** have less tendency to undergo H-aggregation. The absorption maximum of **2a** on the TiO_2 film is a little red-shifted from 439 nm in solution to 445 nm. Dye **2b** displays an absorption maximum at 430 nm, whose peak is not as obvious as

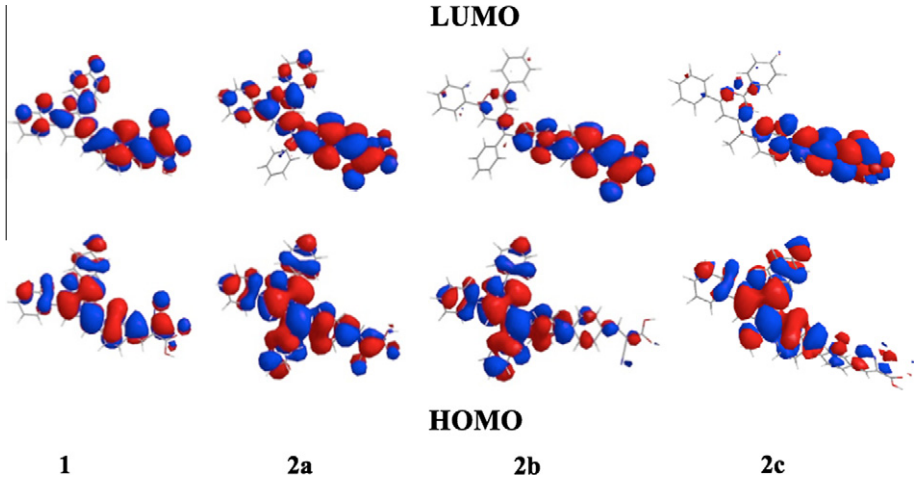

Fig. 2. Frontier molecular orbitals (HOMOs and LUMOs) for **1** and **2a–c** calculated with Gaussian 03 program at the B3LYP/6-31G(d) level.

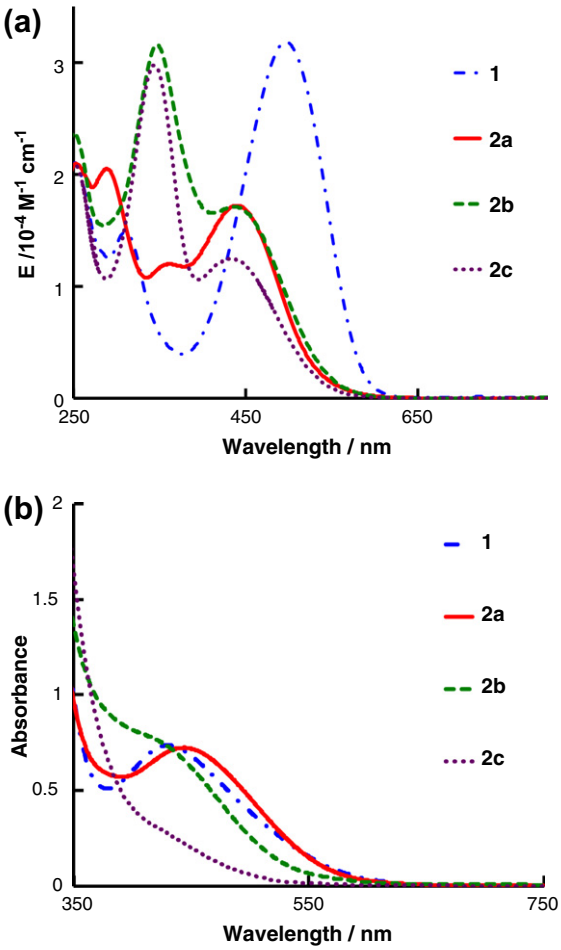

Fig. 3. UV–vis absorption spectra of dyes **1** and **2a–c** in CH_2Cl_2 solution (a) and on 20 nm thick TiO_2 film (b).

Table 1
Photophysical[a] and electrochemical[b] properties of the diphenylpyranylidene dyes in solution.

Dye	**1**	**2a**	**2b**	**2c**
λ_{max} (nm)[a]	497	439	436	433
ε (10^4 M^{-1} cm^{-1})	3.2	1.7	1.7	1.2
E_{0-0} (eV)[c]	2.08	2.09	2.09	2.10
E_{ox} (V vs. NHE)	1.09	0.94	0.89	0.81
E^*_{ox} (V vs. NHE)[d]	−0.99	−1.15	−1.20	−1.29

[a] In CH_2Cl_2.
[b] Measured by cyclic voltammetry in DMF.
[c] Obtained from the edge absorptions.
[d] Estimated by subtracting E_{0-0} from E_{ox}.

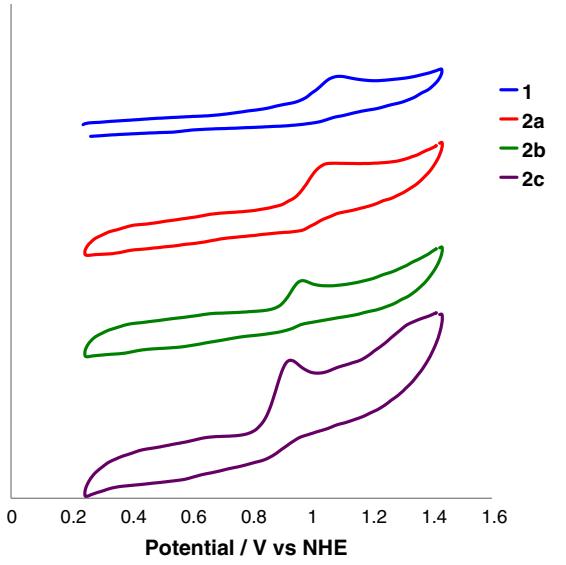

Fig. 4. Cyclic voltammograms of the dyes **1** and **2a–c** in DMF.

that of **2a**. Dye **2c** shows no absorption maximum around the same wavelength.

The redox potentials were measured by cyclic voltammetry in DMF and are listed in Table 1. The cyclic voltammetry curves of the dyes **1** and **2a–c** are shown in Fig 4.

The oxidation potential of **2a** was observed at 0.94 V, which is more negative than that of **1**. The oxidation potential of **2b** is more negative than that of **2a** due to the extended phenyl ring, but is still more positive than the iodine/iodide redox potential value of 0.4 V. The excited states of oxidation potentials of these sensitizers were calculated from the differences between the ground state oxidation potentials and UV–vis absorption onset values [7]. The excited state oxidation potentials of **2a**, **b** are 1.15 V and 1.20 V, respectively, which are more negative than that of **1**. These facts indicate that the electron injection and the electron transfer from I_3^- to the cation-radical state in **2a**, **b** take place more easily than in dye **1**, which is favorable to the application for DSSCs. The oxidation potential of **2c** is negatively shifted due to the stronger electron-donating property of the methyl group.

2.4. Photovoltaic performance

The IPCE spectra for DSSCs based on **2a–c** are shown in Fig. 5. The maximum values of **2a**, **b** are over than 60%. The spectrum of **2a** is broader than that of **2b** and the IPCE values for **2a** are kept high over the wavelength region of 500–600 nm, On the other hand, the maximum value of **2c** decreases to 44% in a narrower wavelength region due to its weak absorption on the TiO_2 thin film as shown in Fig. 3b. The IPCE spectra of **2a–c** are consistent with their absorption spectra in solution and on TiO_2 thin films.

The photovoltaic performances of the DSSCs were measured at 100 mW/cm^2 under simulated AM 1.5 G solar light conditions and listed in Table 2. Fig. 6 illustrates the current density–voltage (I–V) curves plotted for the DSSCs. The photocurrent density (J_{sc}), open circuit voltage (V_{oc}) and fill factor (FF) of **2a** are 10.3 mA cm^{-2}, 0.72 V and 0.72, respectively, leading to an overall conversion efficiency (η) of 5.3%, which is much larger than that of **1** (2.3%). This result indicates that the introduction of the phenyl group is very effective for increasing the conversion efficiency. This is attributed to the suppression of dye-aggregation as well as the protection of approach of I_3^- to the TiO_2. Dye **2b** shows a little decreased efficiency of 4.7% under the same conditions. This is due to the decreased J_{sc} caused by the blue-shift of the IPCE spectrum [8]. The J_{sc} values of **2a**, **b** are twice as high as that of **2c**. This can be explained by their larger extinction coefficients in their absorption spectra resulting in the large IPCE values. Fig. 7 illustrates dark I–V curves of the DSSCs. When the phenyl group was introduced at the vinyl position of the dye **1**, the onset of applied voltage for producing dark current in the DSSC increases from 0.382 to 0.467 and 0.523 V, which leads to the increased open-circuit voltage from 0.51 to 0.72 and 0.73 V. It implies that tri-iodide reductions of DSSC devices based on dyes **2a**, **b** is less likely to occur at the TiO_2 particle surface due to their steric effect. In addition, the V_{oc} values of **2a**, **b** are 0.18–0.19 V greater than that of **2c**. This is due to the greater steric effect arising from the phenyl group compared to the methyl group, which cause the restrained charge recombination between the injected electrons and excited dyes, as well as the suppress of recombination between injected electrons and I_3^- ions [9]. The methyl derivative was not stable in contrast to the phenyl derivatives and the device performance was decreased after standing for 72 h in air.

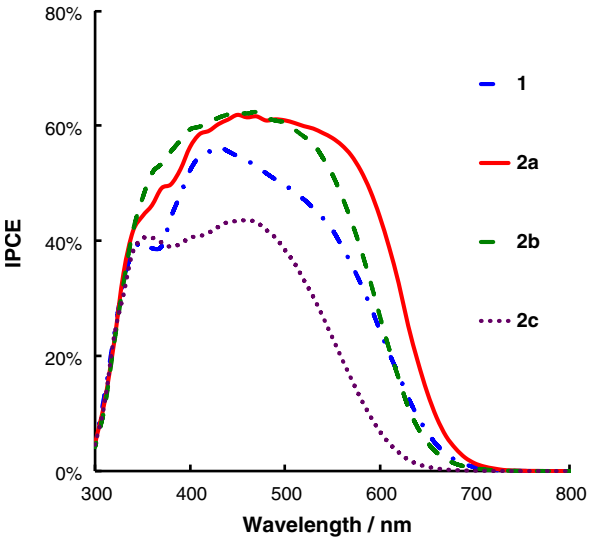

Fig. 5. IPCE action spectra for DSSCs based on **1** and **2a–c**.

Table 2
Photovoltaic performances[a] of the solar cells sensitized with dyes **1** and **2a–c**.

Dye	1	2a	2b	2c
J_{sc} (mA/cm2)	6.5	10.3	8.9	4.9
V_{oc} (V)	0.51	0.72	0.73	0.54
FF	0.70	0.72	0.72	0.72
η (%)	2.3	5.3	4.7	1.9

[a] Illumination: 100 mW cm^2 simulated AM 1.5 G solar light. Electrolyte solution comprised of 0.6 M DMPImI, 0.1 M LiI, 0.2 M I_2 and 0.5 M TBP (in acetonitrile).

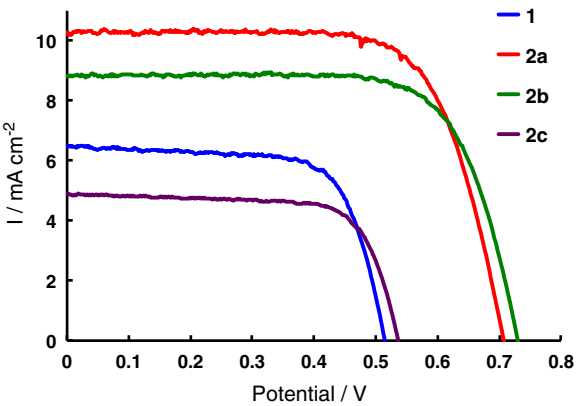

Fig. 6. I–V curves for DSSCs based on **1** and **2a–c** under illumination of 100 mW cm^{-2} AM1.5G simulated light. An aperture mask (0.2399 cm^2) was put on the cells surface to avoid the diffuse light.

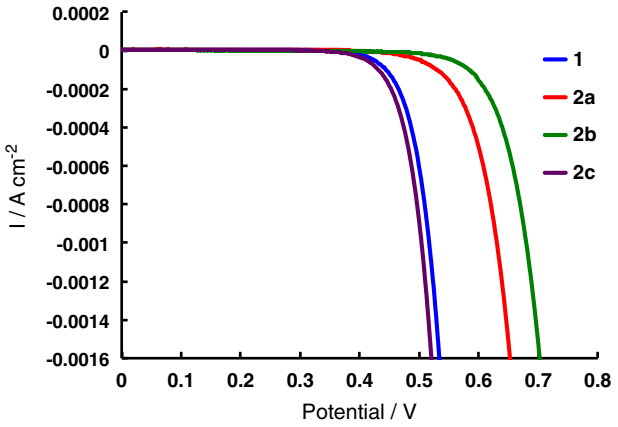

Fig. 7. Dark *I–V* curves for DSSCs based on **1** and **2a–c**.

3. Conclusion

In conclusion, three metal-free organic sensitizers **2a–c** with 2,6-diphenyl-4*H*-pyranylidene unit as donor part were developed. DSSCs based on the phenyl-substituted derivatives **2a**, **b** showed good energy conversion efficiencies of 5.3 and 4.7%, respectively, which are twice than that of **1** without the phenyl substituent under the same conditions. This result shows that the tetraphenylpyranylidene is a promising electron-donor unit for high-efficiency DSSCs. In order to further improve the efficiencies, our next work is focusing on the modification of the diphenylpyranylidene and the spacer units as follows. First, introducing substituents with steric-effect at the termini of 2,6-diphenyl group of the pyran ring will further suppress the dye-aggregation on the TiO_2 surface. Second, well-conjugated π-systems are required as spacer between the donor and acceptor parts for extending the absorption of sensitizer in DSSC. Furthermore, additional anchoring substituents introduced at the phenyl group of the vinyl position will help increase amounts of absorbed dye on the surface of TiO_2 particles.

4. Experimental

4.1. Materials and general procedures

All starting materials and solvents for synthesis, measurements, and solar cell fabrication were purchased from Wako Chemicals, Kanto Chemicals, Tomiyama Pure Chemical Industries Ltd., Aldrich, Tokyo Chemical Industry Co., Ltd., and/or Merck and used without further purification. Melting points were obtained on a Yanaco melting point apparatus and uncorrected. ^{1}H-NMR spectra were recorded on a JEOL JNM-ECP 300 spectrometer and referenced to the residual solvent proton resonance. EI mass spectra were collected on a JEOL JMS-700 mass spectrometer. IR spectra were recorded as KBr disks on a PERKIN ELMER FT-IR Spectrometer PARAGON 1000 spectrophotometer. Elemental analyses were performed at the Tokyo Institute of Technology, Chemical Resources Laboratory. UV–vis spectra were recorded on a JASCO V-650 UV–vis Spectrophotometer. Cyclic voltammetry were recorded on a HOKUTODENKO HZ-5000 containing terabutylammonium hexafluorophoshate (TBAPF6) (0.1 mol dm^{-3}) in dry DMF. The Pt disk, Pt wire and SCE were used as working, counter, and reference electrodes, respectively. Absorption spectra of the dyes on TiO_2 (T20/SP, consisting of 20 nm nanoparticles) film were measured with a SHIMADZU UV- 3101 PC spectrophotometer.

4.2. Synthesis and characterization

4.2.1. 4-((4-Bromophenyl)(phenyl)methylene)-2,6-diphenyl-4H-pyran (*4a*)

Tributyl(2,6-diphenyl-4*H*-pyran-4-yl)phosphonium tetrafluoroborate (**TBDPP**) (0.6 g, 1.15 mmol) dissolved in 30 mL of anhydrous THF was added with *n*-BuLi in hexane solution (0.7 mL, 1.16 mmol) at −78 °C under argon protection. The solution was stirred at −78 °C for 15 min and 4-bromobenzophenone (0.3 g, 1.15 mmol) dissolved in dry THF (10 mL) was added dropwise. The solution was stirred at −78 °C for 30 min and then moved to room temperature and stirred overnight. After the reaction, the solvent was evaporated and the mixture was extracted with dichloromethane and dried over anhydrous sodium sulfate. The residue was purified by column chromatography on silica gel (hexane/dichloromethane = 2/1) to give a yellow solid 0.31 g. Yield: 55%. ^{1}H-NMR (300 MHz, DMSO) δ/ppm = 7.68 (d, 2H), 7.62 (d, 2H), 7.56 (d, 2H), 7.50–7.37 (m, 8H), 7.29 (t, 1H), 7.22–7.14 (m, 4H), 6.61 (s, 1H), 6.56 (s, 1H).

4.2.2. 4-((2,6-Diphenyl-4H-pyran-4-ylidene)(phenyl)methyl) benzaldehyde (*3a*)

Compound **4a** (0.54 g, 1.13 mmol) dissolved in 60 mL of anhydrous THF was added with *n*-BuLi in hexane solution (0.6 mL, 2.26 mmol) at −78 °C under argon protection. The solution was stirred at −78 °C for 2 h and dimethylformamide (0.17 mL, 2.25 mmol) diluted in dry THF (10 mL) was added dropwise. The solution was stirred at −78 °C for 2 h and then moved to room temperature and stirred overnight. After the reaction, the solvent was evaporated and the mixture was extracted with dichloromethane

and dried over anhydrous sodium sulfate. The residue was purified by column chromatography on silica gel (100% dichloromethane) to give a yellow solid 0.096 g. Yield: 20%. ^{1}H-NMR (300 MHz, DMSO) δ/ppm: 9.99 (s, 1H), 7.90 (d, 2H), 7.72 (d, 2H), 7.65 (d, 2H), 7.46 (m, 10H), 7.33 (s, 1H), 7.25 (d, 2H), 6.74 (d, 1H), 6.59 (d, 1H).

4.2.3. (E)-2-Cyano-3-(4-((2,6-diphenyl-4H-pyran-4-ylidene)(phenyl)methyl)phenyl)acrylic acid (**2a**)

To a stirred solution of compound **3a** (0.0294 g, 0.069 mmol) and cyanoacetic acid (0.023 g, 0.27 mmol) in acetonitrile (20 mL) was added piperidine (0.05 g, 0.58 mmol). The reaction mixture was refluxed under argon for 4 h and a yellow precipitate appeared. After cooling the solution to room temperature and filtering precipitate, the crude product was purified through column chromatography on silica gel (dichloromethane/ethanol, 10/1) to give a dark-red solid 0.03 g. Yield: 90%. Mp: 175–185 °C. ^{1}H-NMR (300 MHz, DMSO) δ/ppm = 7.86 (t, 3H), 7.69 (d, 2H), 7.61 (d, 2H), 7.47–7.39 (m, 8H), 7.29 (t, 3H), 7.23 (d, 2H), 6.72 (d, 1H), 6.56 (d, 1H). MS/EI (70 eV): m/z 493 (M^+). Anal. Calcd. for $C_{34}H_{23}NO_3$: C, 82.74; H, 4.70; N, 2.84. Found: C, 82.35; H, 4.33; N, 2.58.

4.2.4. 4′-((2,6-Diphenyl-4H-pyran-4-ylidene)(phenyl)methyl)-[1,1′-biphenyl]-4-carbaldehyde (**3b**)

4a (0.18 g, 0.38 mmol) was dissolved in toluene (20 mL), 1.2 g Na_2CO_3 in 10 mL H_2O and (4-formylphenyl)boronic acid (0.12 g, 0.8 mmol) in ethanolic solution (5 mL) were added. The mixture was deoxygenated under reduced pressure and flushed with argon. $Pd(PPh_3)_4$ (0.017 g) was added and the resulting suspension was heated under reflux for overnight. After cooling to room temperature, ethyl acetate and water were added and the organic phase was separated. The water phase was extracted with ethyl acetate. The combined organic phase was washed with brine, dried over anhydrous sodium sulfate, filtered and evaporated. The product was purified by column chromatography on silica gel (dichloromethane/hexane, 1/2 to 100% dichloromethane) to give an orange solid 0.086 g. Yield: 45%. ^{1}H-NMR (300 MHz, DMSO) δ/ppm: 10.06 (s, 1H), 7.99 (d, 4H), 7.83 (d, 2H), 7.71 (d, 2H), 7.65 (d, 2H), 7.46 (m, 8H), 7.35 (t, 3H), 7.27 (d, 2H), 6.75 (d, 1H), 6.59 (d, 1H).

4.2.5. (E)-2-Cyano-3-(4′-((2,6-diphenyl-4H-pyran-4-ylidene)(phenyl)methyl)-[1,1′-biphenyl]-4-yl)acrylic acid (**2b**)

The similar synthesis and purification to those of compound **2a** gave a dark-red solid. Yield: 92%. Mp: 195–205 °C. ^{1}H-NMR (300 MHz, DMSO) δ/ppm = 8.36 (s, 1H), 8.15 (d, 2H), 7.97 (d, 2H), 7.85 (d, 2H), 7.72–7.63 (m, 4H), 7.48–7.43 (m, 10H), 7.35 (d, 2H), 7.27 (d, 2H), 6.76 (d, 1H), 6.59 (d, 1H). MS/EI (70 eV): m/z 569 (M^+). Anal. Calcd. for $C_{40}H_{27}NO_3$: C, 84.34; H, 4.78; N, 2.46. Found: C, 84.08; H, 4.84; N, 2.31.

4.2.6. 4-(1-(4-Bromophenyl)ethylidene)-2,6-diphenyl-4H-pyran (**4c**)

Tributyl(2,6-diphenyl-4*H*-pyran-4-yl)phosphonium tetrafluoroborate (0.51 g, 0.97 mmol) dissolved in 40 mL of anhydrous THF was added with *n*-BuLi in hexane solution (0.6 mL, 0.99 mmol) at −78 °C under argon. The solution was stirred at −78 °C for 15 min and 4-bromoacetophenone (0.27 g, 1.35 mmol) dissolved in dry THF (15 mL) was added dropwise. The solution was stirred at −78 °C for 30 min and then moved to room temperature and stirred overnight. After the reaction, the solvent was evaporated and the mixture was extracted with dichloromethane and dried over anhydrous sodium sulfate. The residue was purified by column chromatography on silica gel (hexane/dichloromethane = 2/1) to give a yellow solid 0.18 g. Yield: 45%. ^{1}H-NMR (300 MHz, $CDCl_3$) δ/ppm = 7.78 (d, 2H), 7.61 (d, 2H), 7.51–7.35 (m, 8H), 7.20 (d, 2H), 6.53 (s, 1H), 6.47 (s, 1H), 2.14 (s, 3H).

4.2.7. 4′-(1-(2,6-Diphenyl-4H-pyran-4-ylidene)ethyl)-[1,1′-biphenyl]-4-carbaldehyde (**3c**)

The similar synthesis and purification to those of compound **3b** gave a yellow solid. Yield: 39%. ^{1}H-NMR (300 MHz, $CDCl_3$) δ/ppm = 10.07 (s, 1H), 7.97 (d, 2H), 7.84–7.80 (m, 4H), 7.67–7.62 (m, 4H), 7.49–7.30 (m, 8H), 6.61 (s, 1H), 6.58 (s, 1H), 2.21 (s, 3H).

4.2.8. (E)-2-Cyano-3-(4′-(1-(2,6-diphenyl-4H-pyran-4-ylidene)ethyl)-[1,1′-biphenyl]-4-yl)acrylic acid (**2c**)

The similar synthesis and purification to those of compound **2a** gave a dark-red solid. Yield: 43%. Mp: 270–280 °C. ^{1}H-NMR (300 MHz, DMSO) δ/ppm = 8.01 (t, 3H), 7.93–7.87 (m, 4H), 7.81 (d, 2H), 7.62 (d, 2H), 7.53–7.37 (m, 9H), 6.83 (s, 1H), 6.58 (s, 1H), 2.19(s, 3H). Anal. Calcd. for $C_{35}H_{25}NO_3$: C, 82.82; H, 4.96; N, 2.76. Found: C, 82.51; H, 4.65; N, 2.49.

4.3. Fabrication of dye-sensitized solar cells

F-SnO_2 (FTO)-coated glass substrates were cleaned in a detergent solution by an ultrasonic bath, rinsed with water and ethanol, and then dried using N_2 current. Nanocrystalline TiO_2 films of first layer (SOLARONIX Ti-nanoxide T20/SP, consisting of 20 nm nanoparticles) and second layer (SOLARONIX Ti-nanoxide D37/SP, consisting of 37 nm nanoparticles) were prepared using screen-printing technique. After treated by $TiCl_4$, the TiO_2 films were immersed into toluene solution of the dyes (0.3 mM) for about 18 h. The dye-adsorbed TiO_2 film electrode and Pt-counter electrode were assembled into a sealed sandwich solar cell with a hot-melt Surlyn film (30 μm in thickness) as a spacer between the electrodes. A drop of the electrolyte solution {0.6 M 1,2-dimethyl-3-*n*-propylimidazolium iodide (DMPImI) + 0.1 M LiI + 0.2 M I2 + 0.5 M 4-*tert*-butylpyridine (TBP) in acetonitrile} was driven into the cell through the hole in the counter electrode via suction through another drilled hole. Finally, the two holes were sealed using additional hot-melt Surlyn film covered with a thin glass slide.

4.4. Photovoltaic measurements

The prepared dye-sensitized solar cells were illuminated through the conducting glass support with a black mask with an aperture area of 0.2399 cm^2 to avoid the penetrating of diffuse light into the active dye-loaded film (the apparent surface area of the TiO_2 film electrode was

ca. 0.25 cm^2). The performance of the dye-sensitized solar cells was characterized by incident photon-to-current conversion efficiency (IPCE) and photocurrent–voltage (*I–V*) measurements. IPCE were measured with a CEP-99 W system (Bunkoh-Keiki Co., Ltd.). *J–V* curves were obtained from a computer controlled source meter (Advantest, R6243) under illumination of simulated AM 1.5 G solar light from an AM 1.5 solar simulator (Wacom Co., Japan, WXS-80C-3 with a 300 W Xe lamp and an AM 1.5 filter).

Acknowledgements

This work is supported by a Grant-in-Aid for Scientific Research (23350088 and 22550162) from the Ministry of Education, Culture, by Sports, Science and Technology, Japan, and by the Global COE program "Education and Research Center for Emergence of New Molecular Chemistry".

Appendix A. Supplementary data

Supplementary data associated with this article can be found, in the online version, at doi:10.1016/j.orgel.2011.11.020.

References

[1] [a] B. O'Regan, M. Grätzel, Nature 353 (1991) 737;
(b) A. Mishea, M.K.R. Fischer, P. Bäuerle, Angew. Chem. Int. Ed. 48 (2009) 2474;
(c) A. Hagfeldt, G. Boschloo, L. Sun, L. Kloo, H. Pettersson, Chem. Rev. 110 (2010) 6595;
(d) K.C.D. Robson, B.D. Koivisto, A. Yella, B. Sporinova, M.K. Nazeeruddin, T. Baumgartner, M. Grätzel, C.P. Berlinguette, Inorg. Chem. 50 (2011) 5494.

[2] (a) M. Grätzel, J. Photochem. Photobiol. 3 (2004) A164;
(b) M. Grätzel, Inorg. Chem. 44 (2005) 6841;
(c) M.K. Nazeeruddin, F. De Angelis, S. Fantacci, A. Selloni, G. Viscardi, P. Liska, S. Ito, T. Bessho, M. Grätzel, J. Am. Chem. Soc. 127 (2005) 16835;
(d) Y. Chiba, A. Islam, Y. Watanabe, R. Komiya, N. Koide, L. Han, Jpn. J. Appl. Phys. 45 (2006) L638;
(e) B.H. Lee, M.Y. Song, S.Y. Jang, S.M. Jo, S-Y. Kwak, D.Y. Kim, J. Phys. Chem. C 113 (2009) 21453.

[3] (a) K. Hara, K. Sayama, Y. Ohga, A. Shinpo, S. Suga, H. Arakawa, Chem. Commun. (2001) 569;
(b) K. Hara, M. Kurashige, S. Ito, A. Shinpo, S. Suga, K. Sayama, H. Arakawa, Chem. Commun. (2003) 252;
(c) S. Ito, H. Miura, S. Uchida, M. Tanaka, K. Sumioka, P. Liska, P. Comte, P. Pechy, M. Grätzel, Chem. Commun. (2008) 5194;
(d) A. Mishra, M.K.R. Fischer, P. Bäuerle, Angew. Chem. Int. Ed. 48 (2009) 2474;
(e) Y. Ooyama, Y. Harima, Eur. J. Org. Chem. (2009) 2903;
(f) S.S. Park, Y.S. Won, Y.C. Choi, J.H. Kim, Energy & Fuels 23 (2009) 3732;
(g) L.-Y. Lin, C.-H. Tsai, K.-T. Wong, T.-W. Huang, L. Hsieh, S.-H. Liu, H.-W. Lin, C.-C. Wu, S.-H. Chou, S.-H. Chen, A.-I. Tsai, J. Org. Chem. 75 (2010) 4778;
(h) W. Zhu, Y. Wu, S. Wang, W. Li, X. Li, J. Chen, Z. Wang, H. Tian, Adv. Funct. Mater. 21 (2011) 756;
(i) X. Jiang, K.M. Karisson, E. Gabrielsson, E.M.J. Johansson, M. Quintana, L. Sun, G. Boschloo, A. Hagfeldt, Adv. Funct. Mater. 21 (2011) 2944.

[4] (a) A. Bolag, M. Mamada, J. Nishida, Y. Yamashita, Chem. Mater. 21 (2009) 4350;
(b) A. Bolag, J. Nishida, K. Hara, Y. Yamashita, Chem. Lett. 40 (2011) 510.

[5] G.A. Reynolds, F.D. Saeva, J.J. Doney, C.H. Chen, J. Org. Chem. 49 (1984) 4843.

[6] M.K.R. Fischer, S. Wenger, M. Wang, A. Mishra, S.M. Zakeeruddin, Michael Grätzel, Peter Bäuerle, Chem. Mater. 22 (2010) 1836.

[7] (a) X.-H. Zhang, Y. Cui, R. Katoh, N. Koumura, K. Hara, J. Phys. Chem. C 114 (2010) 18283;
(b) S. Qu, W. Wu, J. Hua, C. Kong, Y. Long, H. Tian, J. Phys. Chem. C 114 (2010) 1343.

[8] Z.-S. Wang, N. Koumura, Y. Cui, M. Takahashi, H. Sekiguchi, A. Mori, T. Kubo, A. Furube, K. Hara, Chem. Mater. 20 (2008) 3993.

[9] (a) Z.-M. Tang, T. Lei, K.-J. Jiang, Y.-L. Song, J. Pei, Chem. Asian J. 5 (2010) 1911;
(b) D. Cao, J. Peng, Y. Hong, X. Fang, L. Wang, H. Meier, Org. Lett. 13 (2011) 1610.